RESEARCH PAPER

Formation of fully closed microcapsules as microsensors by microfluidic double emulsion

Bo Wu · Hai-Qing Gong

Abstract Microcapsules templated from microfluidic double emulsions attract a great attention due to their broad new potential applications. We present a method to form transparent polymer microcapsules in small sizes of ∼30 μm with aqueous cores and fully closed shells. We controlled the size ratio of the aqueous core to the polymer shell not only by flow rates of the double emulsions, but also by synergetic interaction between surfactants at the interface of immiscible fluids. We also found that fully closed shells can be formed by generating the double emulsion droplets in a jetting regime, in which the aqueous cores are confined centrally in the double emulsion droplets. We demonstrated the formation of barcodes in these microcapsules for multiplexed bioassays. These transparent microcapsules also have wide and high potentials for the development of various microsensors by functionalizing the liquid-state cores with compounds sensitive and responsive to temperature, light or electromagnetic field.

1 Introduction

Double emulsions are liquid systems of host outer droplets nested with inner droplets. Microfluidic techniques provide precise controls on the sizes of the inner and outer droplets and the number of inner droplets in each outer droplet

B. Wu · H.-Q. Gong (✉)
School of Mechanical and Aerospace Engineering,
Nanyang Technological University,
#50 Nanyang Avenue, Singapore 639798, Singapore
e-mail: mhqgong@ntu.edu.sg

(Utada et al. 2005; Okushima et al. 2004; Nie et al. 2005; Panizza et al. 2008), which extend the applications of double emulsion in drug delivery (Ichikawa and Fukumori 2000; Priest et al. 2008), biological screening (Mastrobattista et al. 2005; Guo et al. 2012) and, especially, manufacture of optical microelements and microsensors (Yang et al. 2006). For example, the monodispersed transparent polymer microcapsules containing charged or magnetic nanoparticles in their liquid cores can be used as pixel units for high-resolution display (Zhu et al. 2011). However, the formation of the transparent polymer microcapsules with the liquid cores is still a challenge. To stabilize the double emulsion droplets, surfactants are dissolved in the three phases of double emulsion in high concentrations. But the double emulsion droplets still easily break up after collection and before solidification of their outer droplets. Instead of using the surfactants, dispersing nanoparticles in the middle-phase polymer precursor is a more effective approach to stabilize the double emulsion droplets with a long time duration up to hours (Chen et al. 2011). Unfortunately, these solidified polymer shells doped with the nanoparticles in high volume fractions may scatter and absorb light significantly, which are not suitable to form the microsensors read out by optical signals.

In this paper, we present a method to form the transparent polymer microcapsules with aqueous cores and fully closed shells by UV-induced polymerization of polymer precursor outer droplets immediately after generation of unstable water-in-oil-in-water (W/O/W) double emulsion droplets in a microfluidic device. Parameter studies on flow rates of three phases and surfactant concentrations in the aqueous inner droplets were made to control the size ratios of the aqueous cores to the polymer shells. Particularly, we found an effective approach to form fully closed microcapsules by generating the double emulsion in a jetting

regime which confined the inner droplets centrally in their outer droplets. We also demonstrated the use of the graphical information of microcapsules to enhance the coding capacity of colorimetric barcodes formed in these microcapsules. These transparent microcapsules have wide and high potentials to create various microsensors by functionalizing their liquid-state cores.

2 Experimental

2.1 Microfluidic device

Figure 1a illustrates the design of the microfluidic device to form the microcapsules, which consists of a T-junction, a Y-junction and a serpentine section. The microfluidic device made by soft lithography of polydimethylsiloxane (PDMS) (Sylgard 184, Dow Corning, USA) was used to form colorimetric barcodes in our previous work (Wu and Gong 2012). The dimensions of microchannels are labeled in Fig. 1b, c). To form the W/O/W double emulsion, the serpentine section downstream of the Y-junction was modified to be hydrophilic and the T-junction maintained hydrophobic. To suspend the double emulsion droplets spherically in the serpentine section, the microchannel downstream of the Y-junction was made with a square cross section which was higher than the microchannels at the T-junction. (See detailed fabrication processes and parameters in Supplementary Materials.)

2.2 Preparation of microcapsules

As illustrated in Fig. 1d, the microcapsules were formed in a three-step process. Firstly, the water-in-oil (W/O) emulsion occurred at the T-junction and the inner droplets of aqueous solution were generated in a flow of ethoxylated trimethylolpropane triacrylate (ETPTA) polymer precursor. Secondly, the inner droplets were engulfed by the outer droplets of ETPTA polymer precursor at the Y-junction to form the W/O/W double emulsion droplets in a flow of sodium dodecyl sulfate (SDS) solution. Finally, the ETPTA outer droplets were solidified by UV light from a mercury lamp equipped to an inverted microscope (Eclipse Ti, Nikon, Japan) to form the microcapsules in the serpentine section. The aqueous solution, the ETPTA polymer precursor and the SDS solution were the inner-phase, middle-phase and outer-phase fluids of the W/O/W double emulsion, respectively. The inner-phase fluid was prepared by adding red or blue food dye in deionized water. The middle-phase fluid was the ETPTA polymer precursor (viscosity: 90 mPa s) added with 4 % (w/v) Daracure 1173 and 2 % (w/v) surfactant of sorbitan monooleate (Span 80). The outer-phase fluid was prepared by adding 2 % (w/w)

SDS in deionized water. The three fluids of the W/O/W double emulsion were injected into the microfluidic device by three syringe pumps, independently.

Carboxyethylsilanetriol sodium (CES) (25 % aqueous solution, Gelest, USA) was used to functionalize the polymer microcapsules with carboxyl groups. Firstly, 100 mg of the microcapsules was washed by ethanol to remove the uncured ETPTA monomer and the surfactants over the outer surfaces of the microcapsules. Then, the microcapsules were rinsed by 10 mM sodium phosphate buffer (PBS buffer, pH 7.4) added with 0.01 % (w/v) SDS with vortex mixing three times. Secondly, the microcapsules were suspended in 5 mL of the PBS buffer added with 500 μL of the CES with gentle mixing for 4 h at room temperature. Finally, the microcapsules were washed by deionized water three times.

2.3 Characterization

The processes of the droplet generations at the T-junction and the Y-junction were observed and recorded by a high-speed camera (Fastcam APX-RS, Photron, Japan) mounted to the inverted microscope. The bright-field micrographs of microcapsules were captured by a monochromatic CCD camera (RETIGE EXi, Qimaging, Canada) mounted on the microscope. A scanning electron microscope (SEM) (JSM-5600LV, JEOL, Japan) was used to capture SEM micrographs of the microcapsules.

3 Results and discussion

3.1 Microfluidic operation

The mechanisms of droplet generations at the T-junction and the Y-junction are mainly governed by the capillary number, $Ca = \eta_c Q_c / \sigma S$, which describes the competition between viscous force and interfacial tension (Gupta et al. 2009; Liu and Zhang 2009; Anna et al. 2003; Lee et al. 2009; de Menech et al. 2008; Utada et al. 2007), in which η_c is the viscosity of the continuing phase fluid, Q_c is the flow rate of the continuing phase fluid, σ is the interfacial tension between the immiscible fluids, and S is the microchannel cross-section area. To control the morphology of the microcapsules templated from the double emulsion droplets, we firstly investigated the generation of W/O emulsion at the T-junction and the generation of W/O/W double emulsion at the Y-junction.

At the hydrophobic T-junction, the continuing phase was the ETPTA polymer precursor and the dispersing phase was the aqueous inner-phase fluid. As shown in Fig. 2a, the volumes of the inner droplets were controlled by the flow rate of the middle-phase ETPTA polymer precursor (Q_m) in

Fig. 1 a Design of the microchannel network to form the microcapsules. **b** Micrograph of the T-junction. **c** Micrograph of the Y-junction. **d** Schematic diagram of the microcapsule formation
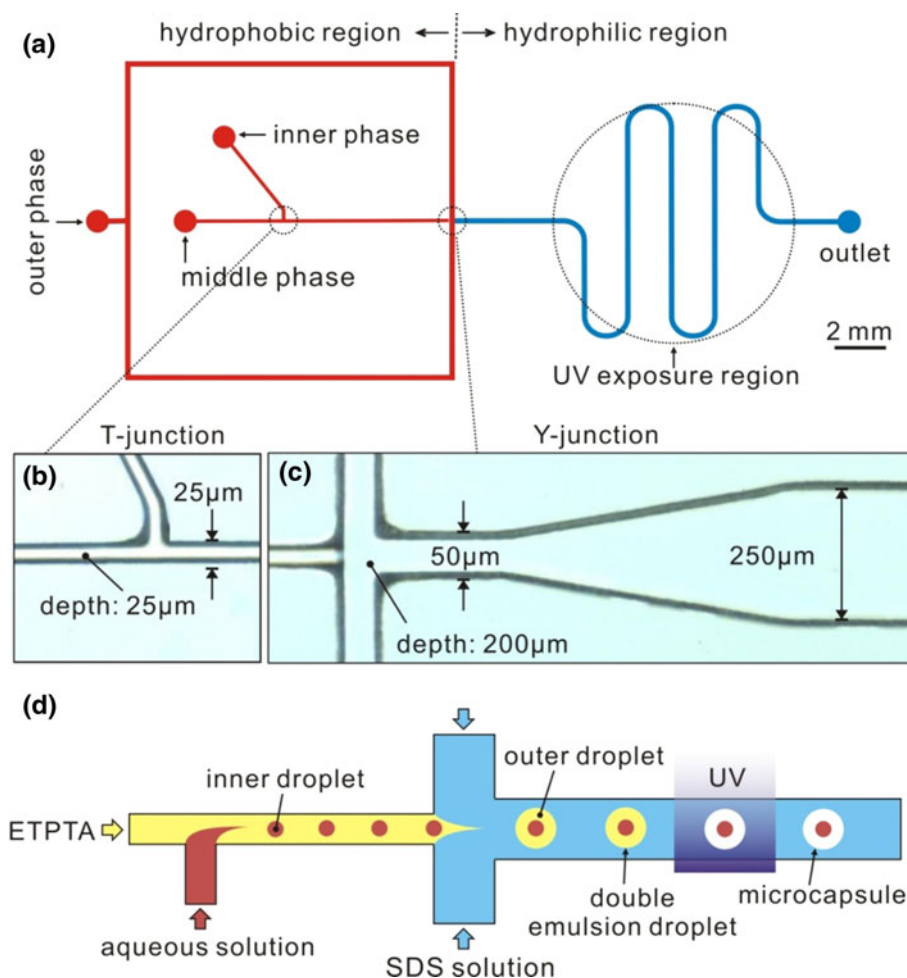
three distinct regimes, including a squeezing regime, a dripping regime and a jetting regime. The flow rate of the inner-phase fluid (Q_i) was set at 0.02 mL h^{-1}, constantly. When the Q_m was 0.01 mL h^{-1}, the inner droplets were generated in the squeezing regime. The red-dyed water filled the microchannel as slugs till the pressure of the ETPTA polymer precursor at the T-junction was high enough to push the slugs forward. The volume of the inner droplet was only determined by the geometry of the microchannel and the ratio of Q_m to Q_i. Increasing Q_m to 0.03 mL h^{-1}, the W/O emulsion began to transfer from the squeezing regime to the dripping regime, in which the shear stress at the interface of the two immiscible fluids became important gradually. The volumes of the inner droplets were changed slightly in a relatively large range of Q_m, while the intervals between them extended apparently with Q_m as shown in Fig. 2b2–b5. Further increasing Q_m to 0.08 mL h^{-1}, the W/O emulsion transferred from the dripping regime to the jetting regime. A jet of the red-dyed water downstream of the T-junction produced spherical inner droplets in the ETPTA flow as shown in Fig. 2b6, b7. It is should be noted that the transfers between the droplet

generation regimes occurred gradually in narrow flow-rate ranges. The flow rate data of vertical dotted lines which separate the three droplet generation regimes in Fig. 2a were approximates.

We found that the volumes of the inner droplets can also be controlled effectively by a little addition of SDS in the aqueous inner-phase fluid, as shown in Fig. 3a. The size ratio of the inner droplet to the outer droplet (d_{inner}/d_{outer}) can be controlled flexibly by combining the two approaches of adjusting Q_m and the altering SDS concentration in the inner-phase fluid. For the double emulsion droplet, d_{inner}/d_{outer} can be represented by $\left(\frac{Q_i}{Q_i+Q_m}\right)^{-1/3}$ (Hennequin et al. 2009). If only Q_m is used to control d_{inner}/d_{outer}, a smaller inner droplet must be encapsulated in a relatively larger outer droplet. Using the synergistic interaction between the nonionic polymeric surfactant of Span 80 and the anionic surfactant of SDS at the oil–water interface (Pons et al. 1997), the interfacial tension between the two immiscible fluids can be reduced significantly by adding a little amount of SDS in the inner-phase fluid. Here, Q_i and Q_m were set at 0.02 and 0.06 mL h^{-1}, respectively. Five
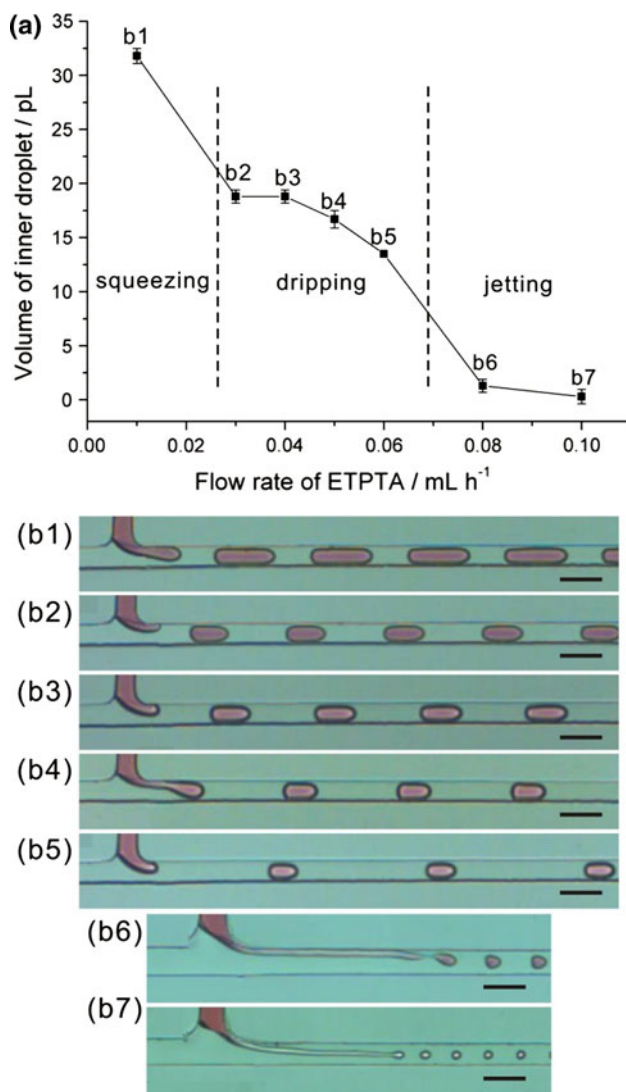
Fig. 2 **a** Volumes of the inner droplets controlled by Q_m. *b1* The W/O emulsion in the squeezing regime. *b2–b5* The W/O emissions in the dripping regime. *b6, b7* The W/O emulsions in the jetting regime. Q_i was 0.02 mL h^{-1}, constantly. The *scale bars* in *b1–b7* are 50 μm in length

Fig. 3 **a** Volumes of the inner droplets controlled by the concentrations of SDS in the inner-phase fluid. Q_i was 0.02 mL h^{-1} and Q_m was 0.06 mL h^{-1}. The SDS concentrations in the inner-phase fluid increased from 0 to 0.04 % in an increment of 0.01 % in *b1–c*. *b1* The W/O emulsion in the dripping regime. *b2* The W/O emulsion started to transfer from the dripping regime to the jetting regime. *b3, b4* The W/O emulsions in the jetting regime. *c* A parallel flow of the inner-phase red-dyed water with the middle-phase ETPTA polymer precursor. The *scale bars* are 50 μm in length

inner-phase fluids of the red-dyed water were prepared by adding SDS in concentrations from 0 to 0.04 % (w/w) in an increment of 0.01 %. Firstly, the inner droplets containing no SDS were formed in the dripping regime as shown in Fig. 3b1. Increasing the SDS concentration to 0.01 %, the W/O emulsion at the T-junction began to transfer from the dripping regime to the jetting regime. A short jet of the red-dyed water emerged downstream of the T-junction as shown in Fig. 3b2. The jet of the red-dyed water produced smaller inner droplet by adding more SDS as shown in Fig. 3b3, b4. However, 0.04 % SDS in the inner-phase fluid failed to form the W/O emulsion. The jet of red-dyed water went gradually to the Y-junction and formed a parallel flow with the ETPTA polymer precursor as shown in
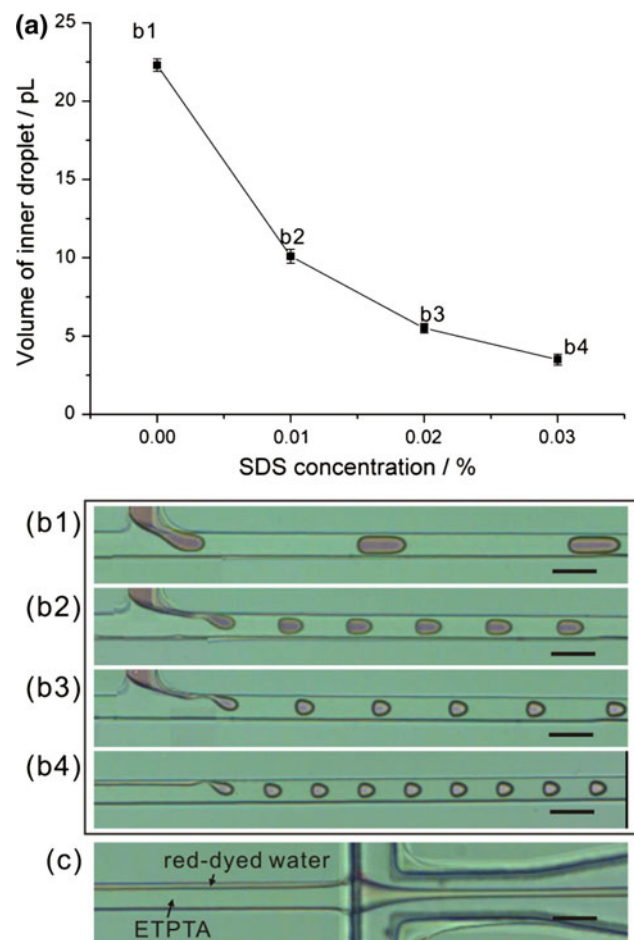
Fig. 3c. The addition of SDS in the aqueous inner-phase fluid not only reduced the interfacial tension between the two immiscible fluids, but also decreased the contact angle of the aqueous inner-phase fluid on the PDMS wall of the microchannel. The red-dyed water added with 0.04 % SDS was no longer a dispersing phase but one more continuing phase.

At the hydrophilic Y-junction, the ETPTA polymer precursor turned to be the dispersing phase and the continuing phase was the outer-phase SDS solution. As shown in Fig. 4, each double emulsion droplet can be formed with multiple inner droplets. The generation frequency of the double emulsion droplets were controlled by the flow rates of the outer-phase fluid of SDS solution (Q_o). The number of the inner droplets in each outer droplet was
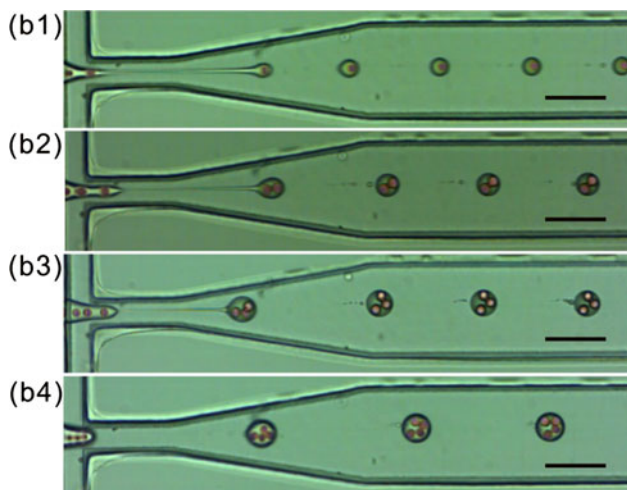
Fig. 4 Number of the inner droplets in individual outer droplets controlled by Q_o. Q_i was 0.02 mL h^{-1} and Q_m was 0.08 mL h^{-1}. Q_o were 5.5, 4.0, 2.8 and 2.5 mL h^{-1} in **a–d**, respectively. The *scale bars* are 100 μm in length

the ratio of the inner droplet generation frequency at the T-junction to the double emulsion generation frequency at the Y-junction.

3.2 Formation of fully closed microcapsules

The outer droplets of ETPTA polymer precursor were cured as the rigid polymer shells to form the microcapsules in the serpentine section under UV exposure. Due to the low shrinkage of ETPTA upon polymerization (~ 11 %), no obvious size difference between the microcapsules and their double emulsion templates was observed. We found that the position of the inner droplet inside the outer droplet

plays a more significant role than d_{inner}/d_{outer} in the formation of the fully closed shells. In equilibrium state, the position of a droplet to a second immiscible droplet in a third immiscible fluid is determined by the interfacial tensions between them (Torza and Mason 1969). Because of the relatively high viscosity of ETPTA, the positions of the aqueous inner droplets in the ETPTA outer droplets maintained the same after the double emulsion droplets detaching from the Y-junction. When the aqueous inner droplet was at the periphery of the ETPTA outer droplet, the thin layer of ETPTA was not cured due to the inhibition of oxygen in the aqueous fluids to UV-induced polymerization. As a result, circular pores were left on the cured polymer shells as shown in Fig. 5a, and the contents in the aqueous cores were leaked. The thinnest shell formed was about 0.6 μm as indicated in Fig. 5b.

We found an effective approach to form the fully closed shells by generating the double emulsion droplets in the jetting regime, in which the aqueous inner droplets were confined centrally inside the ETPTA outer droplets. As shown in Fig. 6a, the double emulsion was formed in the dripping regime when Q_m and Q_o were 0.06 and 4.5 mL h^{-1}, respectively. The inner droplets came to the Y-junction and slowed down at the end of the ETPTA flow region. Each ETPTA outer droplet developed gradually and detached from the ETPTA stream to form a complete double emulsion droplet. Due to the velocity difference between the emerging ETPTA outer droplet and the flow of the outer-phase SDS solution, the shear stress at their interface caused an internal circulating flow inside the ETPTA outer droplet, which forced the aqueous inner droplet towards the periphery of the ETPTA outer droplet. The ETPTA outer droplet with the off-centered
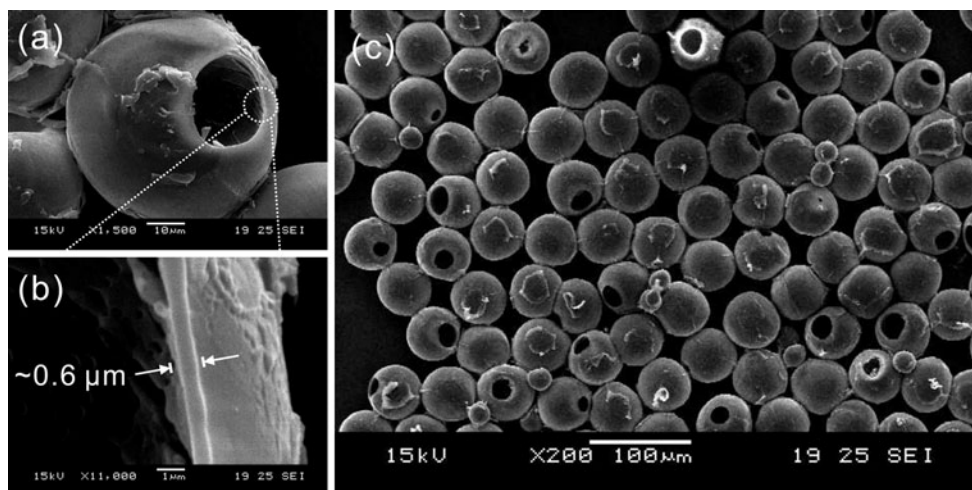

Fig. 5 **a** SEM micrograph of a leaked microcapsule with a circular pore. **b** The thinnest polymer shell was about 0.6 μm. **c** SEM micrograph of the microcapsules templated from the double emulsion droplets generated in the dripping regime

Fig. 6 Image sequences of the double emulsion generation processes. **a** The double emulsion in the dripping regime. Q_i was 0.02 mL h^{-1}, Q_m was 0.06 mL h^{-1}, and Q_o was 4.5 mL h^{-1}. **b** The double emulsion in the jetting regime. Q_i was 0.02 mL h^{-1}, Q_m was 0.08 mL h^{-1}, Q_o was 6.2 mL h^{-1}. The time interval between images is 1.6 ms
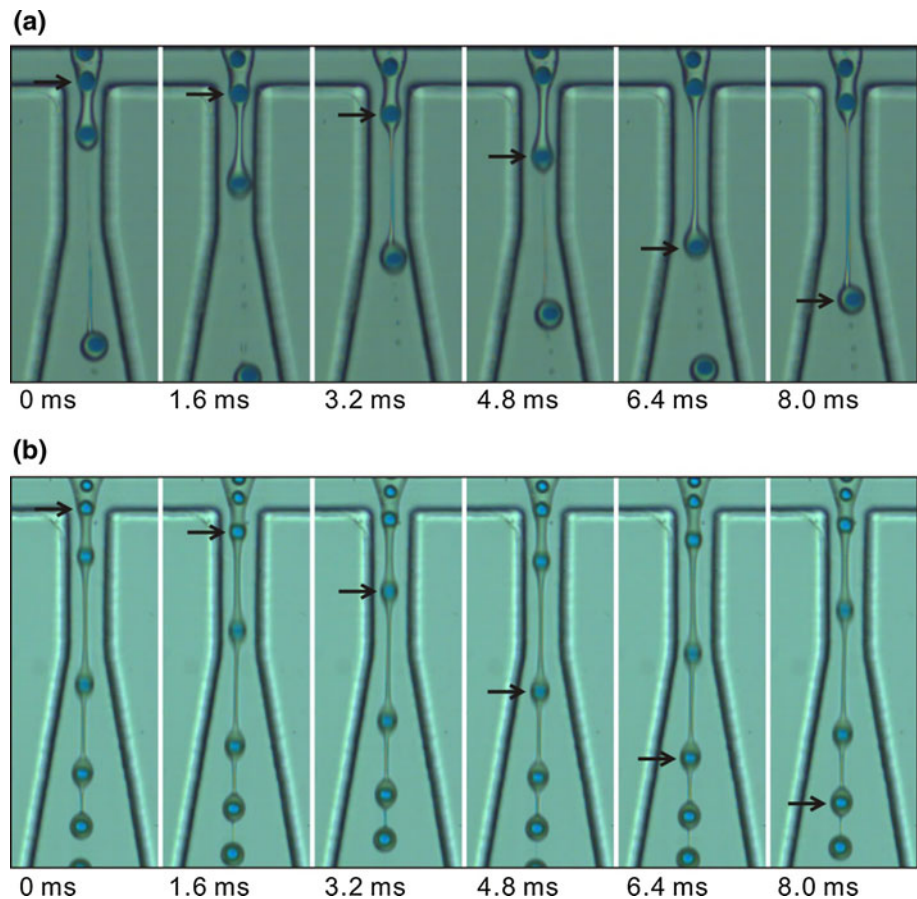
aqueous inner droplet was cured as the polymer shells with the pores. The unstable double emulsion droplets even broke up immediately at the Y-junction, if the aqueous inner droplet was located extremely close to the interface between the ETPTA and the outer-phase SDS solution. In a word, the formation of the fully closed shell is a random incident if the microcapsules are templated from the double emulsion droplets generated in the dripping regime, as shown in Fig. 5c. Further increasing Q_m and Q_o to 0.08 and 6.2 mL h^{-1}, respectively, the double emulsion was formed in the jetting regime as shown in Fig. 6b. The double emulsion in the jetting regime generated the droplet emulsion droplets due to the Rayleigh–Plateau hydrodynamic instability (Lin and Reitz 1998) of the ETPTA jet in the flow of SDS solution. A jet of ETPTA stream broke up into segments containing the inner droplets individually. The segments of the ETPTA jet in the same velocity of the flow of SDS solution confined the inner droplets centrally and turned to the spherical ETPTA outer droplets by reducing their surface areas. The dyed aqueous inner droplets were fully encapsulated by the polymer shells without leakage as shown in Fig. 7a.

3.3 Formation of microsensors

Our previous work demonstrated the formation of colorimetric quantum-dot barcodes in the microcapsules for multiplexed bioassays (Wu and Gong 2012). Actually, these microcapsules can not only be encoded by colorimetric information of dyes or fluorophores in their aqueous cores, but also the graphical information of core sizes and numbers to enhance the coding capacity. As shown in Fig. 7b, the microcapsules with different numbers of cores can be regarded as different spot patterns. Advantageous over pattern barcodes formed by photolithography (Pregibon et al. 2007), the spot patterns formed in the microcapsules do not require photomasks and expensive alignment instruments.

A critical step to bring the barcodes to practical usage is to modify the surfaces of microcapsules with functional groups for optimal bioconjugation to different biomolecules. The polymer surfaces were functionalized with carboxyl groups and amine groups by silane compounds of CET and 3-aminopropyltrimethoxysilane (APTS), respectively (Hermanson 2008). Another simpler method is to mix the monomers with functional groups in the host
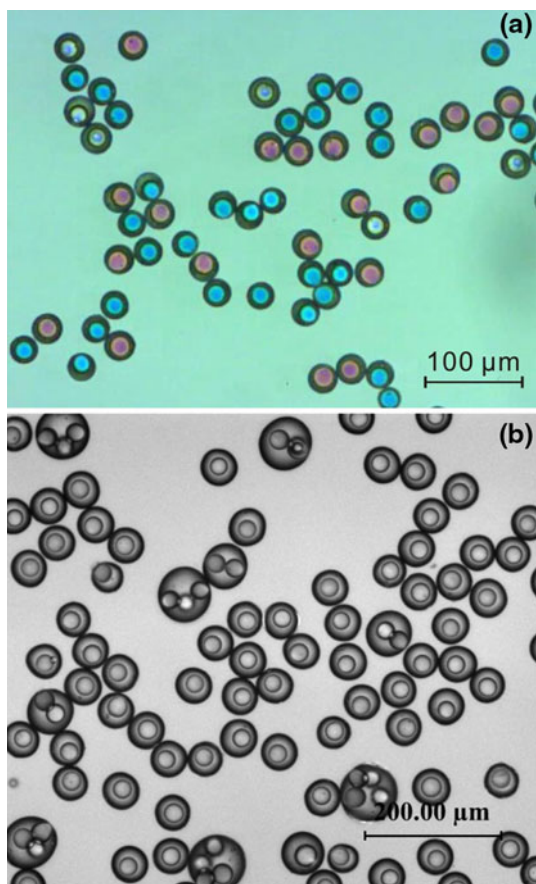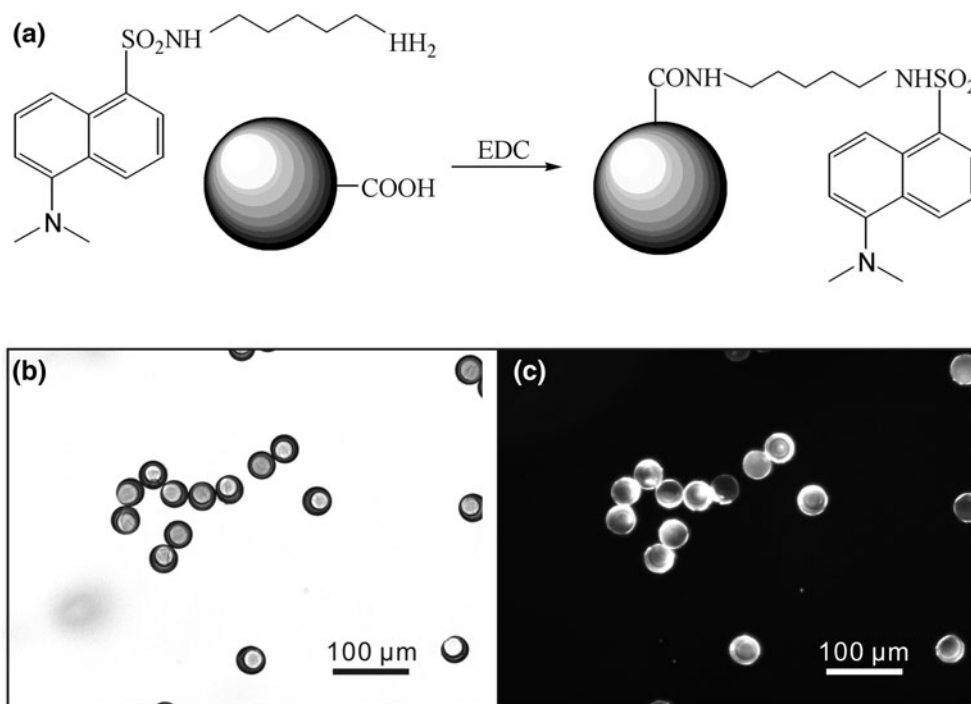
Fig. 7 a Fully closed microcapsules with the red- and blue-dyed aqueous cores. **b** Microcapsules with different numbers of aqueous cores were templated from the double emulsion droplets in Fig. 4a–d (color figure online)

polymer precursor directly (Lewis et al. 2005). The presence of the functional groups on the polymer microcapsules was determined by specific labeling of fluorophore (Ivanov et al. 1996). As illustrated in Fig. 8a, the carboxyl groups on the polymer microcapsules were indicated by labeling dansylcadaverine through a carbodiimide reaction. Figure 8b, c shows the typical bright-field and fluorescent micrographs of the carboxyl-functional microcapsules labeled with dansylcadaverine, respectively. With help of 1-ethyl-3-(3-dimethylaminopropyl) carbodiimide hydrochloride (EDC), oligos modified with amine groups at $5'$ end can be immobilized covalently on the carboxyl-functional microcapsule as probes for multiplexed detection or measurement of target oligos.

Since the microfluidic method to form the microcapsules by the UV-induced polymerization can maintain the original characteristics of compounds encapsulated in the aqueous cores, a variety of microsensors can be developed by functionalizing the liquid-state cores of microcapsules. For example, the transparent polymer microcapsules can be used as thermometers by adding temperature-sensitive dye, Rhodamine-B (Karstens and Kobs 1980), in their aqueous cores. Adding the photochromic compound of bisthienylethene (Tian and Wang 2007) in the aqueous cores, the microcapsules turn to be UV-light sensors. Optical switches or polarisers can also be created by adding liquid crystals in the aqueous cores of microcapsules. It is worth mentioning that thermally unstable compounds can be encapsulated in the microcapsules intactly because the microcapsule formation process has no obvious temperature change.

Fig. 8 a Determination of the carboxyl groups on the microcapsules by specific labeling of dansylcadaverine. **b** Bright-field micrograph of the carboxyl-functional microcapsules labeled with dansylcadaverine. **c** Fluorescent micrograph of the carboxyl-functional microcapsules labeled with dansylcadaverine

4 Conclusion

In summary, we present a method to form fully closed transparent microcapsules with aqueous cores and polymer shells with diameter of $\sim 30\ \mu m$ by UV-induced polymerization of the unstable W/O/W double emulsion droplets in a microfluidic device. The size ratios of the aqueous cores to the polymer shells were controlled by flow rates and the synergetic interaction at the oil–water interface. We found an effective approach to form the fully closed polymer shells by generating the double emulsion templates in the jetting regime, in which the inner droplets are located in the centers of the outer droplets. We also demonstrated the formation of barcodes in the microcapsules using their graphical information of the size and number of aqueous cores to enhance the coding capacity control. The microfluidic method we present can fabricate hundreds of the microcapsules per second, which can be used as excellent host vehicles to develop various microsensors by functionalizing their liquid-state cores.

References

Anna SL, Bontoux N, Stone HA (2003) Formation of dispersions using "flow focusing" in microchannels. Appl Phys Lett 82(3):364–366. doi:10.1063/1.1537519

Chen PW, Erb RM, Studart AR (2011) Designer polymer-based microcapsules made using microfluidics. Langmuir 28(1):144–152. doi:10.1021/la203088u

de Menech M, Garstecki P, Jousse F, Stone HA (2008) Transition from squeezing to dripping in a microfluidic T-shaped junction. J Fluid Mech 595:141–161. doi:10.1017/S002211200700910X

Guo MT, Rotem A, Heyman JA, Weitz DA (2012) Droplet microfluidics for high-throughput biological assays. Lab Chip 12(12):2146–2155. doi:10.1039/C2LC21147E

Gupta A, Murshed SMS, Kumar R (2009) Droplet formation and stability of flows in a microfluidic T-junction. Appl Phys Lett 94 (16):164107. doi:10.1063/1.3116089

Hennequin Y, Pannacci N, de Torres CP, Tetradis-Meris G, Chapuliot S, Bouchaud E, Tabeling P (2009) Synthesizing microcapsules with controlled geometrical and mechanical properties with microfluidic double emulsion technology. Langmuir 25(14):7857–7861. doi:10.1021/la9004449

Hermanson GT (2008) Bioconjugate techniques. Elsevier Academic Press, Amsterdam

Ichikawa H, Fukumori Y (2000) A novel positively thermosensitive controlled-release microcapsule with membrane of nano-sized poly(N-isopropylacrylamide) gel dispersed in ethylcellulose matrix. J Control Release 63(1–2):107–119. doi:10.1016/S0168-3659(99)00181-9

Ivanov VB, Behnisch J, Hollander A, Mehdorn F, Zimmermann H (1996) Determination of functional groups on polymer surfaces using fluorescence labelling. Surf Interface Anal 24(4):257–262. doi:10.1002/(sici)1096-9918(199604)24:4<257:aid-sia107>3.3.co;2-t

Karstens T, Kobs K (1980) Rhodamine-b and rhodamine-101 as reference substances for fluorescence quantum yield measurements. J Phys Chem 84(14):1871–1872. doi:10.1021/j100451a030

Lee W, Walker LM, Anna SL (2009) Role of geometry and fluid properties in droplet and thread formation processes in planar flow focusing. Phys Fluids 21(3):14. doi:10.1063/1.3081407

Lewis PC, Graham RR, Nie ZH, Xu SQ, Seo M, Kumacheva E (2005) Continuous synthesis of copolymer particles in microfluidic reactors. Macromolecules 38(10):4536–4538. doi:10.1021/ma050101n

Lin SP, Reitz RD (1998) Drop and spray formation from a liquid jet. Annu Rev Fluid Mech 30:85–105. doi:10.1146/annurev.fluid.30.1.85

Liu HH, Zhang YH (2009) Droplet formation in a T-shaped microfluidic junction. J Appl Phys 106(3):034906. doi:10.1063/1.3187831

Mastrobattista E, Taly V, Chanudet E, Treacy P, Kelly BT, Griffiths AD (2005) High-throughput screening of enzyme libraries: in vitro evolution of a β-galactosidase by fluorescence-activated sorting of double emulsions. Chem Biol 12(12):1291–1300. doi:10.1016/j.chembiol.2005.09.016

Nie ZH, Xu SQ, Seo M, Lewis PC, Kumacheva E (2005) Polymer particles with various shapes and morphologies produced in continuous microfluidic reactors. J Am Chem Soc 127(22):8058–8063. doi:10.1021/ja042494w

Okushima S, Nisisako T, Torii T, Higuchi T (2004) Controlled production of monodisperse double emulsions by two-step droplet breakup in microfluidic devices. Langmuir 20(23):9905–9908. doi:10.1021/la0480336

Panizza P, Engl W, Hany C, Backov R (2008) Controlled production of hierarchically organized large emulsions and particles using assemblies on line of co-axial flow devices. Colloid Surf A Physicochem Eng Asp 312(1):24–31. doi:10.1016/j.colsurfa.2007.06.026

Pons R, Taylor P, Tadros TF (1997) Investigation of the interactions in emulsions stabilized by a polymeric surfactant and its mixtures with an anionic surfactant. Colloid Polym Sci 275(8):769–776. doi:10.1007/s003960050146

Pregibon DC, Toner M, Doyle PS (2007) Multifunctional encoded particles for high-throughput biomolecule analysis. Science 315(5817):1393–1396. doi:10.1126/science.1134929

Priest C, Quinn A, Postma A, Zelikin AN, Ralston J, Caruso F (2008) Microfluidic polymer multilayer adsorption on liquid crystal droplets for microcapsule synthesis. Lab Chip 8(12):2182–2187. doi:10.1039/b808826h

Tian H, Wang S (2007) Photochromic bisthienylethene as multifunction switches. Chem Commun 8:781–792. doi:10.1039/b610004j

Torza S, Mason SG (1969) Coalescence of 2 immiscible liquid drops. Science 163(3869):813–814. doi:10.1126/science.163.3869.813

Utada AS, Lorenceau E, Link DR, Kaplan PD, Stone HA, Weitz DA (2005) Monodisperse double emulsions generated from a microcapillary device. Science 308(5721):537–541. doi:10.1126/science.1109164

Utada AS, Fernandez-Nieves A, Stone HA, Weitz DA (2007) Dripping to jetting transitions in coflowing liquid streams. Phys Rev Lett 99 (9). doi:10.1103/PhysRevLett.99.094502

Wu B, Gong H-Q (2012) Fluorescence-profile pre-definable quantum-dot barcodes in liquid-core microcapsules. Microfluid Nanofluid 1–9. doi:10.1007/s10404-012-1009-4

Yang H, Han YH, Zhao XW, Nagai K, Gu ZZ (2006) Thermal responsive microlens arrays. Appl Phys Lett 89(11):3. doi:10.1063/1.2354435

Zhu C, Xu WY, Chen LS, Zhang WD, Xu H, Gu ZZ (2011) Magnetochromatic microcapsule arrays for displays. Adv Funct Mater 21(11):2043–2048. doi:10.1002/adfm.201002296